

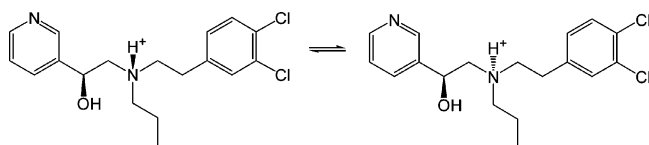
Synthesis, Conformation, and Stereodynamics of a Salt of 2-{[2-(3,4-Dichlorophenyl)ethyl]propylamino}-1-pyridin-3-ylethanol

Tina Korošec,[†] Jože Grdadolnik,[‡] Uroš Urleb,[†] Darko Kocjan,[†] and Simona Golič Grdadolnik^{*‡}

Drug Discovery, Lek Pharmaceuticals d. d., Verovškova 57, SI-1526 Ljubljana, Slovenia, and Laboratory for Molecular Modeling and NMR Spectroscopy, National Institute of Chemistry, Hajdrihova 19, SI-1001 Ljubljana, Slovenia

simona.grdadolnik@ki.si

Received July 14, 2005



A novel synthetic route was developed for 2-{[2-(3,4-dichlorophenyl)ethyl]propylamino}-1-pyridin-3-ylethanol (**4**). A dynamic process due to nitrogen inversion at the central amine nitrogen has been identified by NMR spectroscopy for the dihydrobromide salt of this compound. The conformational properties of the diastereomeric pair were determined by analysis of NOE connectivities and MO calculations.

A series of novel derivatives of pyridylethanol(phenethyl)-amines was synthesized in order to explore the pharmacophoric role of the pyridine nucleus within the tertiary arylalkylamine structure. Such compounds display high affinities for various receptors, a notable example is the inhibition of cholesterol biosynthesis by 2-{[2-(3,4-dichlorophenyl)ethyl]propylamino}-1-pyridin-3-ylethanol (**4**) in a cell assay.¹ In a continuation of our previous work, we have developed an additional synthetic route which considerably improves the overall synthetic yield.

The dihydrobromide salt of **4** has shown some interesting NMR spectral properties. Here we report on a novel synthetic route for the above compound and a detailed investigation of the dynamic and conformational properties of its salt form using NMR spectroscopy and MO calculations.

In the original route,¹ amide **3** was prepared by coupling secondary amine² **2** with the corresponding carboxylic acid using EDC and HOBt activation.³ Tertiary amide **3** was further reduced by a borane–dimethyl sulfide complex⁴ to provide the free base **4** (total yield: 26%) (Scheme 1).

[†] Lek Pharmaceuticals d. d.

[‡] National Institute of Chemistry.

(1) Rode, B.; Rozman, D.; Fon Tacer, K.; Kocjan, D. PCT WO 2004/007456 A1.

(2) Polo, F. L. *Farm. Ed. Sc.* **1963**, *18*, 972–980.

(3) Feng, D. M.; Gardell, S. J.; Lewis, S. D.; Bock, M. G.; Chen, Z.; Freidinger, R. M.; Naylor-Olsen, A. M.; Ramjit, H. G.; Woltmann, R.; Baskin, E. P.; Lynch, J. J.; Lucas, R.; Shafer, J. A.; Dancheck, K. B.; Chen, I. W.; Mao, S. S.; Krueger, J. A.; Hare, T. R.; Mulichak, A. M.; Vacca, J. P. *J. Med. Chem.* **1997**, *40*, 3726–3733.

(4) Brown, H. C.; Choi, Y. M.; Narasimhan, S. *J. Org. Chem.* **1982**, *47*, 3153–3163.

The new method is a reductive alkylation of the secondary amine² **6** using the selective hydride reducing agent sodium triacetoxyborohydride.⁵ The second method gives **4** in higher yield and with fewer side products (total yield: 59%) (Scheme 2). The dihydrobromide salt **5** is prepared in both cases (Figure 1).

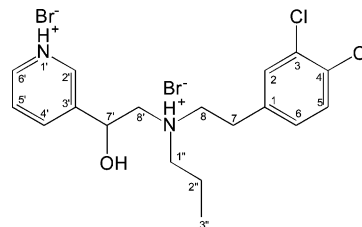


FIGURE 1. Primary structure of **5** illustrating the atom nomenclature used in this study.

The observed extensive line broadening in the proton NMR spectra of **5** measured in DMSO-*d*₆ at room temperature indicates the existence of a dynamic process which could be quantitatively examined by NMR spectroscopy.

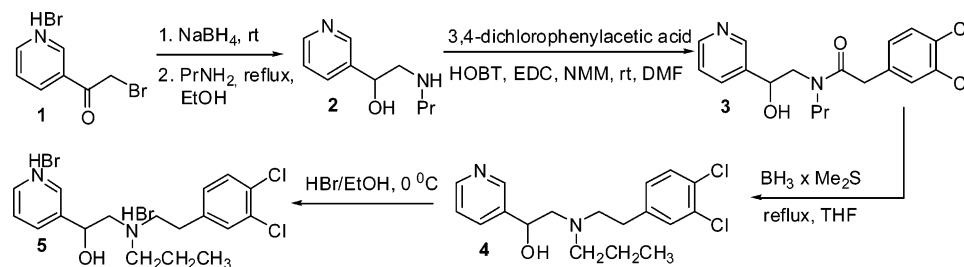
The stereodynamics of tertiary amines is a complex process because the inversion of nitrogen and the rotation around various single bonds are potentially dynamic processes. Although the inversion rates of amines in crowded molecules are usually higher than the rotation rates around single bonds, it is often difficult to distinguish between the two processes. Sometimes the introduction of appropriate substituents influences the magnitude of the inversion or rotation barrier and leads to identification of a particular dynamic process. In open-chain amines, observation of nitrogen inversion is especially difficult because of low activation energies. However, the presence of acidic media can significantly increase the barrier to nitrogen inversion due to N-atom protonation and proton exchange, thus enabling detection of this dynamic process under experimental conditions appropriate for the application of high-resolution NMR techniques.⁶

The dynamic behavior of **5** was further studied in CD₃OD to enable measurements at lower temperatures. Splitting of broad resonances was expected upon cooling the sample, because internal motion is halted on the NMR time scale at sufficiently low temperature, and therefore, separate signals for the present isomers could be observed. Surprisingly, the splitting of resonances in the proton spectrum of **5** in CD₃OD could already be observed at 25 °C (Figure S1, Supporting Information). In its salt form, racemic **4** shows distinctive diastereomeric effects. We suppose that nitrogen inversion is the mechanism responsible for such a dynamic process. A significantly increased barrier to nitrogen inversion, which usually cannot be observed at room temperature in open-chain amines, can be attributed to the presence of HBr. Signal intensities of one diastereomer are slightly weaker, with approximately 10% lower integral values, which indicates a 10% lower population of this diastereomer. The ¹H and ¹³C chemical shift assignment is available in the Supporting Information.

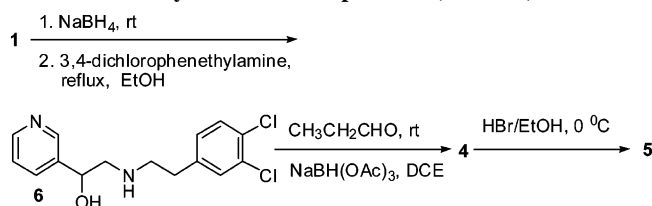
(5) Abdel-Magid, A. F.; Carson, K. G.; Harris, B. D.; Maryanoff, C. A.; Shah, R. D. *J. Org. Chem.* **1996**, *61*, 3849–3862.

(6) Oki, M. In *Application of Dynamic NMR Spectroscopy to Organic Chemistry*; Marchand, A. P., Ed.; Methods in Stereochemical Analysis 4; VCH Publishers: Deerfield Beach, FL, 1985; pp 339–356.

SCHEME 1. Synthesis of Compound 5 (Route A)



SCHEME 2. Synthesis of Compound 5 (Route B)



Chemical exchange signals between the two sets of signals are observed in the NOESY (Figure S2, Supporting Information) and ROESY spectra, which confirm the existence of two exchanging isomers of **5**. In addition, the variable-temperature measurements in CD₃OD show behavior typical of resonances undergoing exchange processes. The broadening and coalescence of signals was observed on heating of the sample (Figure S3, Supporting Information).

Inspection of the carbon chemical shift differences between the diastereomers supports nitrogen inversion as the responsible exchange process. Namely, the resonances of the carbons (C8 and C1'') near the nitrogen atom are largely split. The behavior of the proton resonances is more complex. Large splitting of the resonances of protons H1'', H8, and H8' near the amine nitrogen is in good agreement with nitrogen inversion. On the other hand, comparable splitting of the ortho protons of the dichlorophenyl ring (H2, H6) is unexpected, if it is only the configuration at the amine nitrogen that is responsible for the chemical shift differences between the two diastereomers. The resonances of the pyridine ring are not split. We suppose that the two diastereomers have different overall conformations. The whole exchange process between diastereomers consists of acid dissociation, nitrogen inversion, nitrogen reprotonation, and conformational reorganization.

Barriers (ΔG^\ddagger) of internal motion in **5** were estimated from the differences in the chemical shifts of the two exchange sites at the coalescence temperature. The coalescence of N-bonded carbons (C8 and C1'') is reached at 60 °C, and the barrier is 16.0 kcal mol⁻¹. The extensive overlap of resonances of the protons nearest to the amine nitrogen (H8, H8', H1'') prevents their application for determination of inversion barriers. The signals in the nonoverlapped regions of the proton spectra, which are remote from the amine nitrogen, provide similar barriers of internal motion. The barriers for the H3'', H7', and the ortho protons of the dichlorophenyl ring (H2, H6) are 16.2 (42 °C), 16.4 (40 °C), and 16.6 (52 °C) kcal mol⁻¹, respectively. These results indicate that the exchange process observed in the resonances throughout the molecule is caused mainly by nitrogen inversion at the central amine nitrogen.

The observation of nitrogen inversion at unusually high temperatures is further confirmed by titration studies with benzenesulfonic acid which is used instead of HBr due to its convenience

in the preparation of NMR samples. Benzenesulfonic acid is added in steps of 2 mM to the 10 mM solution of **4** in CD₃OD. Splitting of resonances appears at a 1:1 concentration ratio of acid relative to **4** (Figure S4, Supporting Information). The same resonances are affected as for **5** in CD₃OD. This is a clear indication that nitrogen inversion is the responsible dynamic mechanism. At sufficient acid concentration, the on/off rate of ligation of the acid to the nitrogen lone pair is reduced and the barrier to nitrogen inversion is increased to an extent which enables the observation of separate signals of each diastereomer in the NMR spectra at relatively high temperatures.

Conformational properties of **5** were examined by 2D NOESY and ROESY NMR methods and MO calculations. Although the rate of exchange between diastereomers of **5** in CD₃OD is slow on the NMR time scale at 25 °C and allows observation of separate signals in the NMR spectra, common NOE peaks for both diastereomers are observed in the NOESY spectra at this temperature. NOE measurements were repeated at lower temperature in order to reduce the rate of internal motions. The exchange rate is sufficiently reduced by cooling the sample to 0 °C, since averaging of NOEs is eliminated and each diastereomer has individual NOE cross-peaks (Figure S5, Supporting Information). Thus, observation of conformational differences between diastereomers is enabled at this temperature.

The only difference between the diastereomers that can be observed in the NOESY and ROESY spectra are the NOE cross-peaks of the H7' protons (Figure S6, Supporting Information). One diastereomer has an NOE cross-peak between the H7' and H2'' protons, while the other has it between H7' and H7 protons. This can be attributed to the close proximity of the H7 proton with propyl chain in one and with the ethyl chain in the other diastereomer and indicates a different spatial arrangement of the ethanol, propyl and ethyl chains in diastereomers of **5**. Due to the extensive overlap of signals in the region of the H8 and H8' protons, it is not possible to determine any other specific NOE for the particular arrangement of above-mentioned molecular segments. The same exclusive NOE connectivities of each diastereomer of **4** are also observed in the solution of CD₃OD and benzenesulfonic acid at 0 °C.

The large chemical shift differences of H2 and H6 protons of the dichlorophenyl ring between diastereomers cannot be explained on the basis of NOE connectivities. The H2 and H6 protons have NOE cross-peaks only with nearby protons of the ethyl chain (H7 and H8). NOE cross-peaks of these protons are of similar intensities for both diastereomers, which indicates a similar orientation of the dichlorophenyl ring relative to the ethyl chain.

The MO calculated structures of diastereomers of amine N-protonated species **4** with total charge = +1 fall into two distinctive conformational families with respect to the torsional angles τ_1 (C7–C8–N–C8') and τ_2 (C8–N–C8'–C7') = –80/

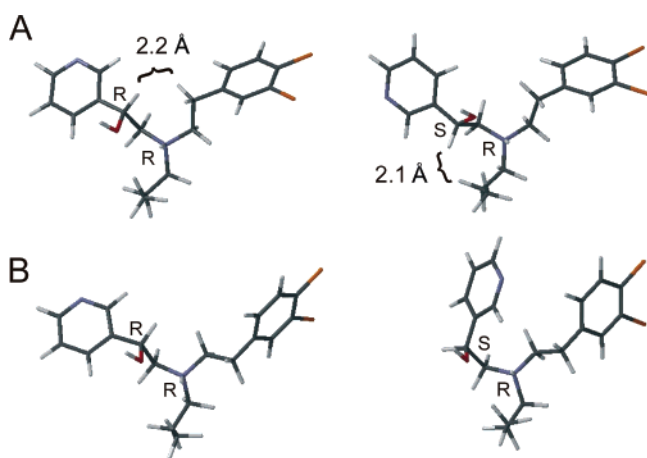


FIGURE 2. Computed structures of diastereomers of amine N-protonated species **4**: (A) conformational family $\tau_1/\tau_2 = -80/150$, (B) conformational family $\tau_1/\tau_2 = -160/90$.

150 and $-160/90$, respectively, with closely spaced potential energy levels.⁷ Molecular orbital calculations in vacuo indicate that the $\text{OH}\cdots\text{NH}^+$ interaction is a dominant feature in both families and that it favors closed structures with the phenyl ring positioned in a π -electron density interaction with the NH^+ group (τ_3 (C1–C7–C8–N) = gauche). Structures with the phenyl ring in an extended conformation (τ_3 = trans) are only 1.5 kcal/mol higher in energy. These structures are more similar to those in polar solvents such as CD_3OD since H7 protons exhibit strong NOE effects.

It was quite interesting to find that both NOE connectivities $\text{H7}'\text{--H7}$ and $\text{H7}'\text{--H2}''$ correspond to the conformational family $\tau_1/\tau_2 = -80/150$ for each diastereomer which exhibit shorter interatomic distances between respective H-atoms than those in the family $\tau_1/\tau_2 = -160/90$ (Figure 2A). On the other hand, the chemical shift differences in protons 2 and 6 between the diastereomers can be explained by the different steric position of the pyridine ring with respect to the phenyl ring within the conformational family $\tau_1/\tau_2 = -160/90$ (Figure 2B). MO calculations confirm the different steric position of H7' protons relative to the propyl and ethyl chain in each diastereomer proposed on the basis of NOE connectivities. Simultaneous observation of the different NOE pattern of H7' protons and the chemical shift differences in protons 2 and 6 of the dichlorophenyl ring between the diastereomers can be explained by the fast conformational exchange between the two conformational families τ_1/τ_2 for each diastereomer in CD_3OD .

We have shown an interesting case of a diastereomeric effect in the salt form of a racemic tertiary arylalkylamine and we have put forward some NMR spectroscopic evidence to demonstrate the mechanisms underlying this effect.

Experimental Section

General Methods. Starting materials, reagents, and solvents were purchased from commercial suppliers and used without further purification. Analytical TLC was performed on silica gel (60 F 254)

(7) We also performed conformational analysis of the diprotonated species and found that the second protonation does not affect the characteristic conformational families. However, it does cause some changes in the distribution of the conformational states. In addition, $\text{p}K_a$'s were determined by Across Barriers (7.66, 4.12), which show that the pyridine nucleus is weakly basic. Therefore, monoprotated species could be predominant, particularly in the organic solvent.

plates (0.25 mm), and components were visualized with ultraviolet light. Column chromatography was carried out on silica gel 60 (particle size 240–400 mesh). Melting points were determined on a hot stage microscope and are uncorrected. IR spectra were recorded with a FT-IR spectrometer. Samples were prepared between NaCl windows or as KBr pellets. MS spectra were measured by ESI, FAB, and HRMS methods. ^1H NMR and ^{13}C NMR experiments for the identification of compounds were carried out at 300 MHz in a CDCl_3 or $\text{DMSO}-d_6$ solution with TMS as the internal standard. The NMR studies of conformation and stereodynamics were carried out at 600 MHz in a CD_3OD solution.

Route A (Scheme 1), 2-Propylamino-1-pyridin-3-ylethanol (2). NaBH_4 (1.0 g, 26.4 mmol) was added to a solution of compd **1** (2.0 g, 7.2 mmol) in anhyd EtOH (40 mL). The reaction mixture was stirred at rt for 2 h. The mixture was filtered, and PrNH_2 (1.4 mL, 17.0 mmol) was added to the filtrate liquid. The solution was heated to reflux and refluxed for 5 h. The EtOH was removed by distillation. The resulting pale yellow solid was dissolved in CHCl_3 (40 mL), the insoluble part was filtered off, and the filtrate was concentrated by distillation under reduced pressure. The product was chromatographed on silica (MeOH/EtOAc, 10:2, and MeOH/ NH_2OH , 9:1) yielding a yellow oil: yield 0.7 g, 54% (93% pure by area % HPLC analysis); ^1H NMR (300 MHz, CDCl_3) δ 0.91 (3H, t, $J = 7.5$ Hz), 1.47–1.59 (2H, m), 2.16–2.93 (3H, m), 2.90 (1H, dd, 1H, $J_{\alpha\text{H}'\text{--}\beta\text{H}} = 3.5$ Hz, $J_g = 11.9$ Hz), 3.45 (2H, br s), 4.82 (1H, dd, $J_{\beta\text{H--}\alpha\text{H}'} = 9.4$ Hz, $J_{\beta\text{H--}\alpha\text{H}'} = 3.4$ Hz), 7.25 (1H, m), 7.73 (1H, td, 1H, $J = 7.6$ Hz, $J = 1.9$ Hz), 8.45 (1H, dd, $J = 4.9$ Hz, $J = 1.5$ Hz), 8.55 (1H, d, $J = 2.25$ Hz); R_f (MeOH/ NH_2OH , 9:1) = 0.70; FT-IR (NaCl) 2963, 1664, 1593, 1470, 1421, 1095, 1053, 903, 809, 719, 634 cm^{-1} ; FAB MS m/z 181 [MH^+]; HRMS m/z calcd for $\text{C}_{10}\text{H}_{16}\text{N}_2\text{O}$ 181.1341, found 181.1345.

2-(3,4-Dichlorophenyl)-N-(2-hydroxy-2-pyridin-3-ylethyl)-N-propylacetamide (3). HOBT (0.41 g, 3.0 mmol) was added to a solution of compd **2** (0.55 g, 3.05 mmol) and 3,4-dichlorophenylacetic acid (0.63 g, 3.0 mmol) in DMF (5 mL). The pH of the solution was adjusted to 8 by adding *N*-methylmorpholine. EDC (0.6 g, 3.1 mmol) was added. After the reaction mixture was stirred at rt overnight, the solvent was evaporated under reduced pressure and the residue dissolved in EtOAc (20 mL). The organic layer was washed with aq saturated NaHCO_3 (20 mL) and NaCl (20 mL) solution and dried (Na_2SO_4). The solvent was evaporated under reduced pressure yielding a colorless oil which was chromatographed on silica (MeOH/EtOAc, 2:10): yield 0.92 g, 82% (99% pure by area % HPLC analysis); ^1H NMR (300 MHz, CDCl_3) δ 0.91 (3H, t, $J = 7.5$ Hz), 1.51–1.63 (2H, m), 3.08–3.33 (2H, m), 3.51 (1H, dd, $J_{\alpha\text{H}'\text{--}\beta\text{H}} = 2.6$ Hz, $J_g = 14.1$ Hz), 3.68–3.75 (3H, m), 4.82 (1H, br s), 5.03 (1H, dd, $J_{\beta\text{H--}\alpha\text{H}'} = 9.4$ Hz, $J_{\beta\text{H--}\alpha\text{H}'} = 3.4$ Hz), 7.11 (1H, dd, $J = 8.3$ Hz, $J = 2.25$ Hz), 7.25–7.44 (3H, m), 7.73 (1H, td, $J = 7.9$ Hz, $J = 1.9$ Hz), 8.45 (1H, dd, $J = 4.75$ Hz, $J = 1.5$ Hz), 8.55 (1H, d, 1H, $J = 2.1$ Hz); R_f ($\text{CH}_2\text{Cl}_2/\text{MeOH}$, 10:0.5) = 0.15; FT-IR (NaCl) 3368, 2965, 2875, 1636, 1472, 1420, 1230, 1131, 1079, 1031, 801, 715 cm^{-1} ; EI MS m/z 366 [M^+], FAB MS m/z 367 [MH^+]; HRMS m/z calcd for $\text{C}_{18}\text{H}_{20}\text{Cl}_2\text{N}_2\text{O}_2$ [M^+] 366.0902, found 366.0910.

2-[[2-(3,4-Dichlorophenyl)ethyl]propylamino]-1-pyridin-3-ylethanol (4). The solution of compd **3** (0.77 g, 2.1 mmol) in dry THF (10 mL) was heated to reflux, and a 2 M solution of borane–dimethyl sulfide complex in diethyl ether (3.30 mL, 6.3 mmol) was added in drops over a 15 min period, allowing dimethyl sulfide to distill off. The reaction mixture was refluxed for 10 h. The THF solution was then hydrolyzed during addition of 6 N HCl (0.35 mL, 2.1 mmol). After 30 min, the clear solution obtained was cooled to room temperature and neutralized with 6 N NaOH (0.6 mL, 3.2 mmol). The reaction mixture was stirred at rt for another 1 h. EtOAc (20 mL) was added, and the organic layer was washed with aq saturated NaHCO_3 (20 mL) and NaCl (20 mL) solution and dried (Na_2SO_4). The solvent was evaporated under reduced pressure to give a product which was further chromatographed on silica

(MeOH/EtOAc, 2:10) to give a colorless oil: yield 0.43 g, 58% (95% pure by area % HPLC analysis); $^1\text{H NMR}$ (300 MHz, CDCl_3) δ 0.91 (3H, t, $J = 7.5$ Hz), 1.48–1.53 (2H, m), 2.46–2.80 (8H, m), 4.63 (1H, dd, 1H, $J_{\beta\text{H}-\alpha\text{H}'} = 10.5$ Hz and $J_{\beta\text{H}-\alpha\text{H}''} = 3.6$ Hz), 7.03 (1H, dd, 1H, $J = 8.2$ Hz, $J = 2.1$ Hz), 7.26–7.38 (3H, m), 7.71 (1H, td, $J = 7.8$ Hz, $J = 1.7$ Hz), 8.52 (1H, dd, $J = 4.75$ Hz, $J = 1.5$ Hz), 8.56 (1H, d, $J = 2.2$ Hz); R_f (MF: MeOH/EtOAc, 2:10) = 0.46; FT-IR (NaCl) 3321, 2963, 2958, 1472, 1425, 1397, 1131, 1030, 819, 715 cm^{-1} ; EI MS m/z 353 [MH^+], FAB MS m/z 353 [MH^+]; HRMS m/z calcd for $\text{C}_{18}\text{H}_{23}\text{Cl}_2\text{N}_2\text{O}$ [MH^+] 353.1187, found 353.1186.

2-[[2-(3,4-Dichlorophenyl)ethyl]propylamino]-1-pyridin-3-ylethanol Dihydrobromide (5). The solution of tertiary amine **4** (0.4 g, 1.1 mmol) in acetone (3.5 mL) was cooled on ice bath. A 0.97 mL (0.22 g HBr, 2.8 mmol) solution of HBr in EtOH was added dropwise. After the precipitate appeared, approximate 2.5 mL of diethyl ether was added. The reaction mixture was stirred on an ice bath for 2 h. The white precipitate was filtered and successively washed with diethyl ether: yield 0.46 g, 79% (99% pure by area % HPLC analysis); mp 130–132 °C; R_f (MF: MeOH/EtOAc, 10:2) = 0.6; $^1\text{H NMR}$ (300 MHz, $\text{DMSO}-d_6$, 50 °C) δ 0.94 (3H, t, $J = 7.1$ Hz), 1.80 (2H, m), 3.10–3.70 (8H, m), 5.54 (1H, m), 7.39 (1H, br), 7.59 (1H, d, $J = 8.2$ Hz), 7.70 (1H, br), 8.11 (1H, dd, $J = 8.1$ Hz, $J = 5.6$ Hz), 8.72 (1H, dt, $J = 8.2$ Hz, $J = 1.7$ Hz), 8.93 (1H, dd, $J = 5.7$ Hz, $J = 1.4$ Hz), 9.09 (1H, d, $J = 1.8$ Hz); FT-IR (KBr) 3411, 3168, 2953, 2684, 1626, 1536, 1472, 1347, 1210, 1128, 1028, 805, 680 cm^{-1} ; EI MS m/z 353 [MH^+], FAB MS m/z 353 [MH^+]; HRMS m/z calcd for $\text{C}_{18}\text{H}_{22}\text{Cl}_2\text{N}_2\text{O}$ [MH^+] 353.1187, found 353.1188. Anal. Calcd for $\text{C}_{18}\text{H}_{24}\text{Br}_2\text{Cl}_2\text{N}_2\text{O} \cdot \frac{4}{3}\text{H}_2\text{O}$: C, 40.83; H, 4.87; N, 5.29. Found: C, 40.86; H, 4.74; N, 5.21.

Route B (Scheme 2). 2-[[2-(3,4-Dichlorophenyl)ethylamino]-1-pyridin-3-ylethanol (6). NaBH_4 (2.0 g, 52.8 mmol) was added to a solution of compd **1** (4.0 g, 14.4 mmol) in anhyd EtOH (60 mL). The reaction mixture was stirred at rt for 2 h. The mixture was filtered, and 3,4-dichlorophenethylamine (3.9 mL, 26.0 mmol) was added to the filtrate liquid. The solution was heated to reflux and refluxed overnight. The EtOH was removed by distillation. The resulting pale yellow solid was dissolved in CHCl_3 (60 mL), the insoluble part was filtered off, and the filtrate concentrated by distillation under reduced pressure. The product was chromatographed on silica (MeOH/EtOAc, 10:2 to gradient elution MeOH/EtOAc, 1:1) to give a yellow oil: yield 3.18 g, 71% (96% pure by area % HPLC analysis); $^1\text{H NMR}$ (300 MHz, CDCl_3) δ 2.66–3.01 (6H, m), 4.71 (1H, dd, $J_{\beta\text{H}-\alpha\text{H}'} = 9.2$ Hz, $J_{\beta\text{H}-\alpha\text{H}''} = 3.6$ Hz), 7.03 (1H, dd, $J = 8.2$ Hz, $J = 2.0$ Hz), 7.26–7.38 (3H, m), 7.70 (1H, td, $J = 7.8$ Hz, $J = 1.8$ Hz), 8.51 (1H, dd, $J = 4.7$ Hz, $J = 1.7$ Hz), 8.56 (1H, d, $J = 2.15$ Hz); R_f (MF: MeOH/EtOAc, 10:2) = 0.3; FT-IR (NaCl) 3411, 2934, 2835, 1602, 1561, 1472, 1413, 1130, 1031, 818 cm^{-1} ; EI MS m/z 311 [MH^+], FAB MS m/z 311 [MH^+]; HRMS m/z calcd for $\text{C}_{15}\text{H}_{17}\text{Cl}_2\text{N}_2\text{O}$ [MH^+] 311.0718, found 311.0725.

2-[[2-(3,4-Dichlorophenyl)ethyl]propylamino]-1-pyridin-3-ylethanol Dihydrobromide (5). Secondary amine **6** (0.5 g, 1.6 mmol) and $\text{CH}_3\text{CH}_2\text{CHO}$ (0.2 mL, 2.4 mmol) were dissolved in 1,2-dichloroethane (10 mL) and then treated with $\text{NaBH}(\text{OAc})_3$ (0.53 g, 2.5 mmol). The mixture was stirred at rt under an Ar atmosphere for 2 h. The reaction mixture was quenched by adding aq saturated NaHCO_3 (20 mL) solution, and the product was extracted with EtOAc (20 mL). The EtOAc extract was dried (Na_2SO_4), and the solvent was evaporated under reduced pressure to give the crude free base **4**, which was chromatographed on silica (MeOH/EtOAc, 10:2) to give a yellow oil: yield 0.47 g, 83% (97% pure by area % HPLC analysis). The product was converted to the dihydrobromide salt **5** (the procedure described under method A was followed).

NMR Studies of Conformation and Stereodynamics. NMR spectra of **4** and **5** were recorded on a 600 MHz NMR spectrometer

in CD_3OD . Sample concentrations were 25 mM and 10 mM. 2D spectra were measured at 25 and 0 °C. The proton chemical shifts were assigned following a standard procedures using homonuclear DQF-COSY,⁸ TOCSY,^{9,10} and NOESY¹¹ experiments in combination with an ^1H – ^{13}C HSQC¹² experiment. Carbons were assigned using the ^1H – ^{13}C HSQC spectrum. Typically, the 2D proton spectra were acquired in the phase sensitive mode with 4096 data points in the t_2 dimension, 4–32 scans, 256–512 complex points in the t_1 dimension, and a relaxation delay of 1–2 s. The ^1H sweep width was 6600 Hz. NOESY and ROESY¹³ spectra were measured with 150 and 300 ms mixing times. The ^1H – ^{13}C HMQC spectrum was acquired as a matrix of 512 × 128 complex points with 4 scans and a relaxation delay of 1 s. The ^{13}C sweep width was 25000 Hz. Data were processed and analyzed using a FELIX software package from Accelrys. Spectra were zero-filled two times and apodized with a squared sine bell function shifted by $\pi/2$ in both dimensions. A linear prediction of the data was applied in the carbon dimension.

The chemical shift differences of the two exchange sites were determined by line shape simulation performed using GRAMS/32 AI software from Thermo Galactic. For accurate determination of the frequencies at coalescence the second derivatives were used. Band components with known frequencies were adjusted using a band fitting algorithm to minimize the difference between the experimental and calculated band shape. A mixture of Lorentzian and Gaussian band shape was used throughout. The only restriction in the band fitting algorithm was the relative intensity of the band component, which was assumed to obey the expected theoretical values.

MO Calculations. Conformational analysis was performed using a Spartan software package running on a Silicon Graphics computer. All rotatable bonds were systematically varied and conformational energies calculated at the AM1 level. Relevant minima were also calculated at the ab initio HF level using a 3-21g* and 6-31g* basis set. The calculations with the 6-31g* basis set were performed using Gaussian 98 software.

Acknowledgment. We thank Silva Zagorc and Sandi Boršček for technical assistance. This work was supported by Lek Pharmaceuticals d.d., the Ministry of Higher Education, Science, and Technology of Slovenia, and the European Community (STEROLTALK project contract No. LSHG-CT-2005-512096).

Supporting Information Available: (1) Table of the ^1H and ^{13}C chemical shift assignments for **5** in CD_3OD , (2) proton spectrum of **5** in CD_3OD , (3) expanded region of the NOESY spectra of **5** in CD_3OD showing the exchange cross-peaks, (4) temperature dependence of selected ^1H NMR signals of **5** in CD_3OD , (5) dependence of selected ^1H NMR signals of **4** upon titration with benzenesulfonic acid, (6) expanded regions of the NOESY spectra of **5** measured at 25 and 0 °C in CD_3OD , (7) expanded region of the ROESY spectra of **5** measured at 0 °C in CD_3OD , and (8) compact Gaussian 98 output of structures presented in Figure 2. This material is available free of charge via the Internet at <http://pubs.acs.org>.

JO051455F

(8) Rance, M.; Sorensen, O. W.; Bodenhausen, G.; Wagner, G.; Ernst, R. R.; Wuethrich K. *Biochem. Biophys. Res. Commun.* **1983**, *117*, 479–485.

(9) Braunschweiler, L.; Ernst, R. R. *J. Magn. Reson.* **1983**, *53*, 521–528.

(10) Bax, A.; Davis, D. G. *J. Magn. Reson.* **1985**, *65*, 355–360.

(11) Jeener, J.; Meier, B. H.; Bachmann, P.; Ernst, R. R. *J. Chem. Phys.* **1979**, *71*, 4546–4553.

(12) Willker, W.; Leibfritz, D.; Kerssebaum, R.; Bermel, W. *Magn. Reson. Chem.* **1993**, *31*, 287–292.

(13) Griesinger, C.; Ernst, R. R. *J. Magn. Reson.* **1987**, *75*, 261–271.